Prescribed-Time Robust Differentiator Design Using Finite Varying Gains

Yury Orlov, Ramón I. Verdés Kairuz, and Luis T. Aguilar, *Senior Member, IEEE*

***Abstract*—A novel hybrid differentiator is proposed for any time-varying signal, whose second derivative is uniformly bounded. The exact real-time differentiation is obtained in prescribed time, and it is based on the robust observer design for the perturbed double integrator. The proposed observer strategy is in successive applications of rescaled and standard supertwisting observers with finite (time-varying and respectively constant) gains. The former observer aims to nullify the observation error dynamics in prescribed time whereas the latter observer is to extend desired robustness features to the infinite horizon. The resulting real-time differentiator uses the current signal measurement only and inherits the observer features of robust convergence to the estimated signal derivative in prescribed time regardless of the initial differentiator state. Tuning conditions to achieve the exact signal differentiation in prescribed time are explicitly derived. Theoretical results are supported by an experimental study of the exact prescribed-time velocity estimation of an oscillating pendulum, operating under uniformly bounded disturbances. The developed approach is additionally discussed to admit an extension to the sequential arbitrary order differentiation.**

***Index Terms*—Prescribed–time stability, robust exact differentiator, time–varying systems, variable structure systems.**

I. Introduction

PRESCRIBED-TIME stabilization is a modern trend in the control area, motivated by applications (e.g., tactical missile guidance), where control objectives should be achieved within a short, finite time. In the pioneering work [1], prescribed-time stabilization was conceptually introduced for nonlinear systems in the normal form. The proposed linear state feedback employed time-varying gains, such as

$$\mu(t) = \frac{T^m}{(T-t)^m},\ m = 1, 2, \ldots, t \in [0, T), \tag{1}$$

Manuscript received March 4, 2021; revised May 10, 2021; accepted May 23, 2021. Date of publication May 27, 2021; date of current version June 28, 2021. This work was supported by the Mexican Council of Science and Technology (CONACYT) under Grant 285279 and Grant A1-S-9270. Recommended by Senior Editor L. Menini. *(Corresponding author: Yury Orlov.)*

Yury Orlov is with the Department of Electronics and Telecomunications, Mexican Scientific and Advanced Studies Center of Ensenada, Ensenada 22860, México (e-mail: yorlov@cicese.mx).

Ramón I. Verdés Kairuz and Luis T. Aguilar are with Instituto Politécnico Nacional—CITEDI, Avenida Instituto Politécnico Nacional, Tijuana 22435, México (e-mail: rverdes@citedi.mx; laguilarb@ipn.mx).

Digital Object Identifier 10.1109/LCSYS.2021.3084134

which became infinitely large as time approached the prescribed convergence time $T > 0$. As a matter of fact, using high gains manifested their implementation problem itself though the control input was shown to remain uniformly bounded.

The baseline design idea of [1] was explicitly centered around a scaling state transformation and implicitly around (i.e., it could readily be interpreted in terms of) the time transformation

$$s(t) = -T \ln \frac{T-t}{T} : [0, T) \to [0, \infty). \tag{2}$$

The above time transformation is obtained by integrating the time-varying gain

$$\mu_1(t) = \frac{T}{T-t}, \quad 0 \le t < T \tag{3}$$

that corresponds to (1), specified with $m = 1$, i.e., it reads $\dot{s} = \mu_1(t)$ and monotonically grows from $\mu_1(0) = 1$ to infinity as $t \to T$. Being typical for high gain and singularly perturbed systems, the transformation stretches the prescribed-time interval $[0, T)$ to the infinite horizon $\mathbb{R}_+ := [0, \infty)$. The standard stability analysis of the transformed system would therefore suffice to conclude the prescribed time stabilization of the underlying non-transformed system.

Later on, the above idea was successfully used to derive prescribed-time observers for systems in the canonical observer form [2] and to prescribed-time observer-based output feedback stabilization for controllable linear systems [3], not necessarily in the normal form [4], and for nonlinear strict feedback systems [5]. Since the prescribed-time controllers and observers were developed with time-varying gains grown unbounded, while the state and observation position error did not decay fully to zero, the robustness of the design remained questionable. Several approaches such as adding a state dead zone, gain saturation, and setting the terminal controller/observer time to exceed the prescribed time, were proposed to address robustness issues. While facilitating practical implementation by preventing unbounded gains, the approaches sacrificed the accuracy of the state and estimation error convergence, see [5, Remark 6].

It should be noted that using the inverse time rescaling

$$t(s) = T(1 - e^{-s/T}) : \mathbb{R}_+ \to [0, T), \tag{4}$$

resulting from (2), one transforms a globally asymptotically stable system into its counterpart which is stabilized in

prescribed time. Apart from (4), any monotonically increasing smooth time transformation, squeezing the infinite time interval $[0, \infty)$ into $[0, T)$ can be used to preserve the prescribed time stabilization.

Based on such an observation, several nonlinear feedback laws were deduced in [6] to exemplify prescribed time stabilization of nonlinear systems. Similar ideas were used in [7] to exploit the time-varying homogeneity, initially introduced in [8], for recasting prescribed-time stabilizing feedback laws from their sliding mode fixed-time stabilizing counterparts. The resulting control algorithms were accompanied with uniformly bounded time-varying gains, thereby admitting their straightforward implementation in practice.

The primary concern of the present work is to extend the robust exact finite-time differentiator [9] to its prescribed-time counterpart. Similar to [9], the current development is reduced to the supertwisting observer design, but reworked in the hybrid setting to meet the prescribed-time convergence. Potential robustness to the measurement noise is another motivation of featuring the supertwisting observer in the hybrid framework to be developed.

At the initial stage, the hybrid observer in question utilizes the rescaled supertwisting modification with time-varying gains. Since the supertwisting observer is finite-time stable over the infinite horizon [10], rescaling it over the prescribed-time interval yields the observer convergence time faster than the prescribed one. Having the faster convergence ensures that the time-varying supertwisting gains remain uniformly bounded at the initial transition stage that precedes the exact state estimation, immediately enforced once the observer starts to evolve in the sliding mode. Right after that, the hybrid observer switches to the standard supertwisting structure with constant gains, thereby robustly tracking the exact state estimation over the infinite horizon in the presence of admissible disturbances.

The resulting robust exact differentiator design forms the *main contribution* of this letter. The design is based on the hybrid supertwisting-flavored prescribed-time observer with finite varying gains. From the implementation standpoint, the developed observer possesses a clear advantage compared to the linear prescribed-time observer [2], designed with infinitely large gains. The design admits an extension to an arbitrary order differentiation, e.g., by the sequential signal differentiation, which would feature, in addition to [11], the exact differentiation not simply in finite time but also in prescribed time. A similar extension is therefore expected to be possible for the prescribed-time observer design for arbitrary order MIMO (multi-input multi-output) systems in the normal form.

The rest of this letter is outlined as follows. Background material is collected in Section II. Observer-based differentiator design is developed in Section III. Theoretical results and their comparison to the existing literature are illustrated in Section IV by conducting a numerical and experimental study of the exact prescribed-time velocity estimation, made for an oscillating pendulum, operating under external disturbances and measurement noise. Finally, Section V concludes this letter with a potential extension to prescribed-time differentiation of an arbitrary order.

II. Preliminaries

For classical stability concepts, used throughout, the reader may refer to the textbook [12]. For later use, other related definitions are summarized below for a generic system

$$\dot{x} = \eta(x, t), \;\; x(t_0) = x^0 \tag{5}$$

with the time variable $t \in \mathbb{R}$, state vector $x(t) \in \mathbb{R}^n$, time derivative $\dot{x}(t) = dx(t)/dt$, and piecewise continuous right-hand side $\eta(x, t)$. Finite time stability of such a system, whose solutions are throughout viewed in the sense of Filippov [13], requires finite-time convergence of its arbitrary solution to an equilibrium. It is formally defined by [8, Definition 2.8] as follows. Let $x = 0$ be an equilibrium of (5).

Definition 1: System (5) is globally finite-time stable in the origin if it is globally asymptotically stable and any solution $x(t, t_0, x^0)$ of (5) is nullified for all $t \geq t_0 + \mathcal{T}(t_0, x^0)$ for some finite $\mathcal{T}(t_0, x^0)$, referred to as the settling time function of the initial conditions t_0, x^0.

According to [14, Definition 2], system (5) is referred to as fixed-time stable if its settling time function is uniformly bounded over the entire domain of initial conditions.

Definition 2: System (5) is globally fixed-time stable in the origin if it is globally finite-time stable and its settling time function $\mathcal{T}(t_0, x^0) \leq T_{\max}$ is bounded by a positive constant $T_{\max}$ for all $t_0 \in \mathbb{R}, x^0 \in \mathbb{R}^n$.

If in addition, a fixed-time stable system can be tuned by means of a control parameter that admits the state convergence to the origin at an arbitrarily small time instant irrespectively of any initial conditions, the system is then referred to be stabilizable in prescribed time.

The sliding mode filter

$$\dot{z} = -\lambda \operatorname{sign}(z(t) - \gamma(t)), \quad z(0) = z^0 \in \mathbb{R}, \tag{6}$$

which is capable of approximate differentiation of a reference signal $\gamma(t)$, is well-known [15] to track $\gamma(t)$ in finite time provided that $|\dot{\gamma}(t)| \leq \gamma_0$ for all $t \geq 0$ and some positive constant $\gamma_0 < \lambda$. Indeed, being rewritten in terms of the deviation $\tilde{z}(t) = z(t) - \gamma(t)$ from the reference signal, (6) takes the form

$$\dot{\tilde{z}} = -\lambda \operatorname{sign} \tilde{z} - \dot{\gamma}(t), \;\; t \geq 0. \tag{7}$$

By differentiating the Lyapunov function $V(\tilde{z}) = |\tilde{z}|$ along the solutions of (7), initialized beyond the origin, one derives $\dot{V} \leq -(\lambda - \gamma_0)$ thereby concluding that (7) arrives in the origin in a settling time $\mathcal{T} \leq \frac{|V(\tilde{z}(0))|}{\lambda - \gamma_0}$ and stays there after that. A motion along the switching surface $\tilde{z} = 0$ is typically referred to as *sliding mode*.

Hence, the finite-time tracking in (6) is ensured in the sliding mode. By the equivalent control method [15], one concludes $\lambda \operatorname{sign} \tilde{z}(t) = \dot{\gamma}(t)$ for $t \geq \mathcal{T}$, so that the finite-time estimation of the time derivative of the reference signal $\gamma(t)$ is achieved. Since in the sliding mode $\tilde{z}(t) = 0$ for $t \geq \mathcal{T}$, the input is switched with high (theoretically, infinite) frequency, its instantaneous average value $u_{eq}(t)$, approximating the signal derivative $\dot{\gamma}$, is normally obtained [15] from a low-pass filter $\kappa \dot{u}_{eq} = -u_{eq} + \lambda \operatorname{sign} \tilde{z}$, $\kappa > 0$, whose arbitrarily initialized output $u_{eq}(t)$ approaches the fast switching input $\lambda \operatorname{sign} \tilde{z}(t)$ for all $t \geq 0$ as $\kappa \to 0$.

The differentiator

$$\dot{z}_1 = z_2 - \lambda_1 \lfloor z_1 - \gamma(t) \rceil^{\frac{1}{2}}, \ \dot{z}_2 = -\lambda_2 \operatorname{sign}(z_1 - \gamma(t)) \quad (8)$$

from [9] is exact (rather than approximate) for a signal $\gamma(t)$, whose second-order time derivative magnitude $|\ddot{\gamma}(t)| \leq \gamma_1$ is uniformly bounded for all $t \geq 0$ by some positive constant $\gamma_1 < \frac{\lambda_1}{2}, \frac{\lambda_1\lambda_2}{1+\lambda_1}$. Hereinafter, the notation

$$\lfloor z_1 \rceil^{\frac{1}{2}} = \sqrt{|z_1|} \operatorname{sign} z_1$$

is used for brevity.

Once rewritten in terms of the signal deviations $\tilde{z}_1(t) = z_1(t) - \gamma(t), \tilde{z}_2(t) = z_2(t) - \dot{\gamma}(t)$, (8) takes the form

$$\dot{\tilde{z}}_1 = \tilde{z}_2 - \lambda_1 \lfloor \tilde{z}_1 \rceil^{\frac{1}{2}}, \ \dot{\tilde{z}}_2 = -\lambda_2 \operatorname{sign} \tilde{z}_1 - \ddot{\gamma}(t) \quad (9)$$

of the supertwisting algorithm which is finite-time stable [16, Th. 5] with a settling time $\tilde{T} > 0$, depending on the initial deviation values. Thus, the exact tracking $z_2(t) = \dot{\gamma}(t)$ of the signal time derivative is ensured in (8) for all $\tilde{T} > 0$.

A hybrid extension of (8), which is moreover fixed-time stable, is given in [17]. Real-time differentiation in prescribed time is developed next.

III. Observer-Based Differentiator Design

The real-time differentiation of a smooth signal is addressed in terms of the robust exact state estimation of the double integrator

$$\dot{x}_1 = x_2, \quad \dot{x}_2 = f(x_1, t) + \phi(x, t), \quad (10)$$

where $t \in \mathbb{R}_+$ is the time variable, $x(t) = (x_1, x_2)^T \in \mathbb{R}^2$ is the state vector, the position $x_1(t)$ is the only available measurement. The integrator is driven by an *a priori* known piece-wise continuous input $f(x_1, t)$ and it is affected by a piece-wise continuous disturbance $\phi(x, t)$ with an *a priori* known magnitude bound $\Phi > 0$ such that

$$|\phi(x, t)| < \Phi \text{ for all } x \in \mathbb{R}^2, t \in \mathbb{R}_+. \quad (11)$$

The main objective of the present work is to exactly estimate the state velocity $x_2(t)$ over the available position measurement $x_1(t)$ within a prescribed time $T > 0$, regardless of the initial conditions and admissible disturbances. Alternatively, the objective might be viewed as to exactly differentiate the signal $x_1(t)$ in prescribed time with the disregarded input $f(x_1, t) = 0$ and with the disturbance term $\phi(x, t)$, standing for measurement imperfections.

The following hybrid observer

$$\begin{aligned} \dot{\xi}_1 &= \xi_2 + G_1(e_1(t), t), \\ \dot{\xi}_2 &= f(x_1(t), t) + G_2(e_1(t), t) \end{aligned} \quad (12)$$

is proposed for the perturbed double integrator (10). Hereinafter, $\xi = (\xi_1, \xi_2)^T$ is the observer state, $e = x - \xi$ is the observation error with the components e_1, e_2,

$$G_1(e_1, t) = \begin{cases} \frac{\mu_1(t)}{T} e_1 + \alpha \sqrt{\mu_1(t)} \lfloor e_1 \rceil^{\frac{1}{2}}, & \text{if } |\operatorname{sign} e_1| = 1 \\ \alpha \lfloor e_1 \rceil^{\frac{1}{2}}, & \text{otherwise,} \end{cases} \quad (13)$$

and

$$G_2(e_1, t) = \begin{cases} \beta \mu_1(t) \operatorname{sign} e_1, & \text{if } |\operatorname{sign} e_1| = 1 \\ \beta \operatorname{sign} e_1, & \text{otherwise} \end{cases} \quad (14)$$

are the observer injection terms with $\mu_1(t)$, given by (3), and $\alpha, \beta > 0$ such that

$$\alpha > 2\Phi \quad \text{and} \quad \beta > (1 + \alpha^{-1})\Phi. \quad (15)$$

The hybrid observer (12) is composed of the supertwisting observer, acting iff $|\operatorname{sign} e_1| \neq 1$, and its time-varying counterpart, confined to the set $e \in \mathbb{R}^2 : |\operatorname{sign} e_1| = 1$. As shown in the observer stability proof below, the time-varying observer component enforces the observation error to reset to zero faster than the prescribed time when it switches to the standard supertwisting observer which keeps the observation error in the sliding mode that occurs in the origin $e_1 = e_2 = 0$ of the error state space once $|\operatorname{sign} e_1| \neq 1$.

By inspection, the error dynamics are governed by

$$\begin{aligned} \dot{e}_1 &= e_2 - G_1(e_1, t), \\ \dot{e}_2 &= \phi(x(t), t) - G_2(e_1, t). \end{aligned} \quad (16)$$

Specifically, the time-varying observer substructure

$$\begin{aligned} \frac{d\xi_1}{dt} &= \xi_2 + \frac{\mu_1(t)}{T} e_1 + \alpha \sqrt{\mu_1(t)} \lfloor e_1 \rceil^{\frac{1}{2}}, \\ \frac{d\xi_2}{dt} &= f(x_1(t), t) + \beta \mu_1(t) \operatorname{sign} e_1 \end{aligned} \quad (17)$$

is pre-composed in such a manner that the corresponding error dynamics

$$\begin{aligned} \frac{de_1}{dt} &= e_2 - \frac{\mu_1(t)}{T} e_1 - \alpha \sqrt{\mu_1(t)} \lfloor e_1 \rceil^{\frac{1}{2}}, \\ \frac{de_2}{dt} &= \phi(x(t), t) - \beta \mu_1(t) \operatorname{sign} e_1 \end{aligned} \quad (18)$$

are deducible from the standard supertwisting system

$$\begin{aligned} \frac{d\varepsilon_1}{ds} &= \varepsilon_2 - \alpha \lfloor \varepsilon_1 \rceil^{\frac{1}{2}}, \\ \frac{d\varepsilon_2}{ds} &= \phi(x(t(s)), t(s)) e^{-s/T} - \beta \operatorname{sign} \varepsilon_1 \end{aligned} \quad (19)$$

by rewriting it in terms of the rescaled time variable (2) and rescaled states

$$\mu_1(t) e_1(t) = \varepsilon_1(s(t)), \ e_2(t) = \varepsilon_2(s(t)). \quad (20)$$

To validate the underlying relation (20) between the error dynamics (18) and (19) for any disturbance applied, the additive perturbation of (19) has deliberately been specified in the form

$$\phi(x(t(s)), t(s)) e^{-s/T} = \frac{\phi(x(t(s)), t(s))}{\mu_1(t(s))}, \quad (21)$$

using the inverse time transformation (4). The magnitude of such a disturbance is estimated $|\phi(x(t(s)), t(s))) e^{-s/T}| < \Phi$ by the upperbound Φ of $|\phi(x(t), t)|$.

By construction, the error dynamics are settled to zero faster than T regardless of any initial conditions and any uniformly bounded disturbance (21). Indeed, the supertwisting dynamics (19) are well-known [16, Th. 5] to vanish in a finite time instant $S_0(\varepsilon_1^0, \varepsilon_2^0, \alpha, \beta, \phi)$ which depends on

the initial values $\varepsilon_1^0 = \varepsilon_1(0), \varepsilon_2^0 = \varepsilon_2(0)$, the supertwisting gains α, β, and the applied disturbance (21). Hence, in the original time variable t, the error dynamics (18) vanish at $T_0(S_0) = T(1 - e^{-S_0/T}) < T$, i.e., before the time-varying gain (3) escapes to infinity at $t = T$. This is the main motivation of using the nonlinear observer instead of the linear prescribed-time observer [2], which faces the implementation problem for the infinite gain (3) when $t \to T$. In addition, the observer robustification over the infinite horizon is obtained.

The switching time instant

$$T_0 = \inf\{t \in [0, T] : \operatorname{sign} e_1(t) \in (-1, 1)\} \tag{22}$$

is clearly associated with the moment $T_0(S_0)$ when the sliding mode occurs in the origin $e_1 = e_2 = 0$. Indeed [16], the supertwisting observer dynamics (19) cross the axis $e_1 = 0$ everywhere but the origin where the second order sliding mode occurs. By the equivalent control method [15], the sign function $\operatorname{sign} e_1(t)$ in (12) takes intermediate values within the interval $(-1, 1)$ in the origin $e_1 = e_2 = 0$ only because otherwise it takes an extremal value 1 or -1. Since $e_2(t)$ is not available to the designer, the only option of switching the observer structure is to automatically make it at the time instant (22) when the sliding mode starts.

The following result is thus established.

Theorem 1: Consider the double integrator (10) and its observer (12)–(15) with an arbitrarily small $T > 0$ independent of initial conditions and admissible disturbances. The error dynamics (16) are then fixed-time stable with the convergence time $T_0 < T$ and with the bounded time-varying gain (3), applied at the initial stage $[0, T_0)$ only.

Proof: By inspection, relation (20) between the error dynamics (18) and (19) is straightforwardly verified for $t \in [0, T_0)$. In other words, the supertwisting system (19) represents the initial behavior of the observer error dynamics (18) for $t \in [0, T_0)$, expressed in the rescaled time (2) and state variables (20). Since the rescaled error dynamics (19) are finite-time stable under the parameter subordination (15) regardless of whichever admissible disturbance affects the dynamics (see [16] for details), it follows that the original error dynamics (18) are robustly finite-time stable, too, with the settling time $T_0 < T$.

Indeed, due to (20) where $\mu_1(t) \geq 1$ by its definition (3), one concludes that $e_1(t) = e_2(t) = 0$ at some $t = T_0(e_1^0, e_2^0, \alpha, \beta, \phi) < T$ that depends on the initial values $e_1^0 = e_1(0), e_2^0 = e_2(0)$, observer gains α, β, and admissible disturbance ϕ. Moreover, (3) remains bounded because it is switched off after T_0.

Thus, at the time instant $t = T_0$, the observer error dynamics (16) switch the injection terms to the standard supertwisting algorithm which rejects admissible disturbances and keeps the error states in the origin for all $t \geq T_0$. This completes the proof of Theorem 1. ∎

IV. Prescribed-Time Velocity Estimation of a Mechanical System

The effectiveness of the proposed derivative estimation is further tested in the simulation study of the prescribed-time observer design for an oscillating pendulum, governed by

$$(Ml^2 + J)\ddot{q} = \tau - f_v\dot{q} - Mgl\sin(q) + d(t). \tag{23}$$

Hereinafter, $q, \dot{q} \in \mathbb{R}$ stand for the angular position and respectively for the angular velocity of the pendulum, M is the mass of the pendulum, l is the distance from its rotation axis to the center of mass, J is the moment of inertia of the pendulum with respect to the center of mass, g is the gravity acceleration, f_v is the viscous friction coefficient, $\tau \in \mathbb{R}$ is the torque produced by the actuator, and $d(t) \in \mathbb{R}$ incorporates external disturbances, affecting the pendulum. The position measurement $q(t) \in \mathbb{R}$ is assumed to be the only available information on the pendulum behavior.

In terms of the state vector $x = (x_1, x_2)^T = (q, \dot{q})^T \in \mathbb{R}^2$, the pendulum model (23) is rewritten as follows

$$\begin{aligned} \dot{x}_1 &= x_2, \\ \dot{x}_2 &= b\big[\tau(t) - f_v x_2 - Mgl\sin x_1 + d(t)\big] \end{aligned} \tag{24}$$

where $b = 1/(Ml^2 + J)$. By denoting

$$f(x_1, t) = b\big[\tau - Mgl\sin x_1\big], \phi(x, t) = b\big[d(t) - f_v x_2\big] \tag{25}$$

in the pendulum model (24), one arrives at the perturbed double integrator form (10). Thus, viewing the viscous friction force $f_v x_2$ as a disturbance of a certain magnitude bound, the prescribed-time observer (12)–(15), specified with (25), yields the desired pendulum state estimate.

TABLE I
Parameter Values of the Laboratory Pendulum

Parameter	Value	Unit
M	0.0474	kg
l	0.11	m
J	3.11×10^{-3}	kg m^2
g	9.81	m/s^2
f_v	2.43×10^{-4}	N s/rad

A. Simulation Results

For the physical meaning, the parameters of the pendulum, used in the subsequent simulations, are drawn from the CITEDI laboratory prototype. The parameter values are collected in Table I.

In the simulations, the pendulum is driven from the origin $x_1(0) = x_2(0) = 0$ by the torque and disturbance inputs, chosen in the form

$$\tau(t) = \frac{a_1}{b} sin(\omega_1^\tau t), \tag{26}$$

$$d(t) = \frac{D}{2b}\Big[\sin(\omega_1^d t) + \cos(\omega_2^d t)\Big] \tag{27}$$

and specified with the parameters

$$a_1 = 10,\ \omega_1^\tau = 4.2,\ D = 1,\ \omega_1^d = 1.57,\ \omega_2^d = 1.26. \tag{28}$$

It is clear that the disturbance term ϕ in (25) admits the following magnitude upperbound

$$|\phi(x, t)| \leq D + bf_v x_2^{max} \text{ for all } x \in \mathbb{R}^2, t \in \mathbb{R}_+ \tag{29}$$

where the maximum possible velocity of the simulated pendulum is *ad hoc* estimated as $x_2^{max} = 7$ rad/s. For the parameter

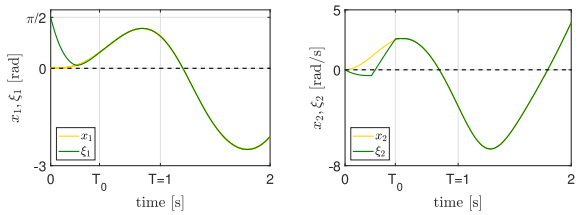

Fig. 1. Simulation results: time responses of the states and the state estimates.

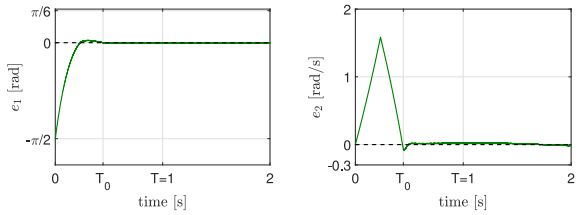

Fig. 2. Simulation results: time responses of the observation errors.

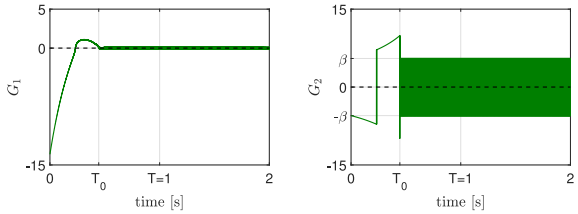

Fig. 3. Simulation results: time responses of the injection terms.

values of Table I, the above upperbound $D + bf_v x_2^{max}$ is thus numerically estimated with $\Phi = 1.46$.

In the simulation runs, observer (12)–(15) of the pendulum model (24)–(29) is initialized with $\xi_1(0) = \frac{\pi}{2}$ rad and $\xi_2(0) = 0$ rad/s, and it is tested in the presence of the measurement noise $\psi(\cdot)$ in the observation channel

$$y(t) = x_1(t) + \psi(t). \tag{30}$$

The noise-corrupted measurement $y(t)$ is modeled with

$$\psi(t) = 10^{-3} \sin(10^4 t), \tag{31}$$

and the resulting measurement (30) is then substituted, for $x_1(t)$, into the observer injection terms (13), (14). Along with this, the observer is specified with the prescribed time $T = 1$ s and the parameters $\alpha = 3.4$, $\beta = 5.5$, chosen to respect the required relations (11), (15).

The simulations are conducted using the Euler forward integration method with the integration step 1×10^{-4} s.

Figure 1 corroborates the prescribed-time convergence of the estimated state of the pendulum to its nominal value in the presence of the measurement noise and the viscous friction force $f_v\dot{q}$, and the modeled disturbance $d(t)$. As clearly seen from Fig. 2, the observation error escapes to zero faster than the prescribed time $T = 1$ s. The injection terms (13) and (14), used in the proposed observer (12), are depicted in Fig. 3, and they are concluded to remain uniformly bounded on the entire time interval, i.e., before and after the prescribed time T.

TABLE II
PT OBSERVER [2, TH. 1]

Injection terms	Parameters
$g_1 = \left(l_1 + 2\frac{m+2}{T}\mu_1\right) e_1, \quad \mu_1(t) := \frac{T}{T-t}$ $g_2 = \left(l_2 + l_1\frac{m+2}{T}\mu_1 + \frac{(m+1)(m+2)}{T^2}\mu_1^2\right) e_1$	$T = 1.005$, $m = 1$, $l_1 = 3$, $l_2 = 2$.

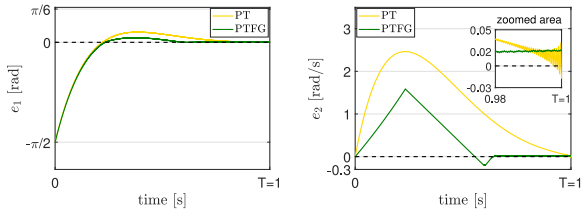

Fig. 4. Comparative simulations: time responses of the PT and PTFG observation errors.

B. Comparative Numerical Study

For the sake of comparison, a prescribed-time observer, recently introduced in [2, Th. 1] and further referred to as *PT observer*, is additionally tested on the same pendulum model. Recall that while being confined to the finite time interval $[0, T)$, the PT observer deals with infinite gains (1) when the time variable t approaches the prescribed time T, thereby yielding numerical precision limitations (see [2, Sec. II-A] for details). This is in contrast to the developed observer (12)–(15), operating with finite time-varying gains on the infinite horizon and yielding the exact robust state estimate not only by the prescribed time instant T but also for all $t \geq T$. For ease of reference, the proposed prescribed-time observer with finite gains is subsequently abbreviated as *PTFG observer*.

Due to the above observations, a fair comparison of the observers is confined to the prescribed-time interval $[0, T)$ while the PT observer works adequately. The comparison is made within the simulation framework of Section IV-A. The PT and PTFG observers are thus tested in the presence of the measurement noise (31) in the observation channel (30) and with the external disturbance (25).

To mitigate the numerical precision limitation problem for the PT observer simulation as time tends to the prescribed moment T and the PT observer gains go to infinity, the prescribed convergence time T is recommended [2, Sec. II-A] to be extended to a larger value. In the simulations of the PT observer, the prescribed time is therefore extended from $T = 1$ s to $T = 1.005$ s for the price of the estimation error convergence to within some neighborhood of the origin. The injection observer terms, designed in [2, Th. 1], are given in Table II with the accompanying parameters, used in the simulations.

Fig. 4 shows the estimation errors of the PT and PTFG observers. A harmful effect of the measurement noise is seen for the PT observer, producing the velocity estimation error $e_2(t)$, diverging near the prescribed time T when the low magnitude noise is magnified by an infinitely large observer gain. Such an undesired effect is however not present for the PTFG observer.

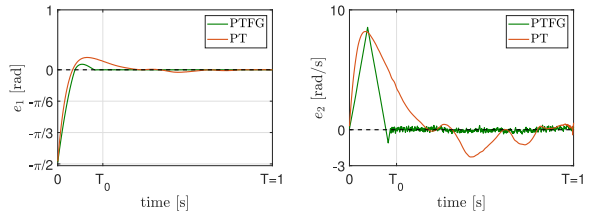

Fig. 5. Experimental comparison: time responses of the PT and PTFG observation errors.

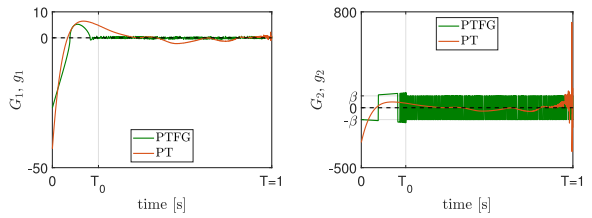

Fig. 6. Experimental comparison: time responses of the PT and PTFG injection terms.

C. Comparative Experimental Study

To add practical value to the present investigation, theoretical results are supported on the experimental setup, consisting of a DC motor manufactured by *Leadshine* and a pendulum prototype with the parameters given in Table I. The motor rotor is equipped with a 1000 ppr optical encoder for the position measurement to feed the observer. Apart from this, the velocity measurement is obtained from the *dSPACE 1701* prototyping hardware, and it is proceeded off-line using low-pass filtering for the only purpose of evaluating the observer performance.

In the experimental study, the prescribed time is again set to $T = 1$ s. As before, the PT observer convergence time is extended to $T = 1.005$ s to avoid an implementation problem. To excite the pendulum dynamics the torque input (26) is applied with the same parameters (28) whereas the external disturbance (27) is disregarded. For achieving an appropriate observer performance, both the PT and PTFG parameters are tuned, by trial and error, to $m = 8$, $l_1 = 8$, $l_2 = 19.3$ and to $\alpha = 13.4$, $\beta = 88$, respectively.

The experiments are conducted with the same observer initial conditions at the upright rest location, used in the simulation stage, whilst the pendulum starts from the origin.

Fig. 5 shows the estimation errors of the PT and PTFG observers. A harmful effect of the model inadequacies and measurement inaccuracy is seen for the PT observer. Such an undesired effect is however not present for the PTFG observer what is achieved for the price of high frequency oscillations, caused by fast switching of the injection terms in the supertwisting observer. The injection terms of the PTFG observer are additionally shown in Fig. 6 to remain bounded during the observation time interval, whereas the injection terms of the PT observer are shown to drastically grow near the prescribed time.

V. Conclusion

A prescribed-time differentiator is developed based on the supertwisting observer design reworked in the hybrid framework that relies on time and state rescaling. The proposed design is shown to be robust for signals with uniformly bounded second order derivatives and it is accompanied with explicitly-given parameter tuning conditions for achieving the robust exact signal differentiation in prescribed time. The design efficiency is supported in numerical and experimental studies carried out for a prescribed-time robust estimate of the velocity of an oscillating pendulum, operating under uniformly bounded disturbances and measurement noise.

The developed approach admits a straightforward extension to the sequential signal differentiation up to order $n \in \mathbb{N}$ provided that all signal derivatives up to order $n+1$ are uniformly bounded. A challenging work in progress is to make such an extension under a less restrictive assumption that only $(n+1)$-th order derivative is uniformly bounded as it has done in [11] with the finite-time (rather than prescribed-time) differentiator convergence.

References

[1] Y. Song, Y. Wang, J. Holloway, and M. Krstic, "Time-varying feedback for regulation of normal-form nonlinear systems in prescribed finite time," *Automatica*, vol. 83, pp. 243–251, Sep. 2017.

[2] J. Holloway and M. Krstic, "Prescribed-time observers for linear systems in observer canonical form," *IEEE Trans. Autom. Control*, vol. 64, no. 9, pp. 3905–3912, Sep. 2019.

[3] J. Holloway and M. Krstic, "Prescribed-time output feedback for linear systems in controllable canonical form," *Automatica*, vol. 107, pp. 77–85, Sep. 2019.

[4] B. Zhou, "Finite-time stabilization of linear systems by bounded linear time-varying feedback," *Automatica*, vol. 113, Mar. 2020, Art. no. 108760.

[5] P. Krishnamurthy, F. Khorrami, and M. Krstic, "A dynamic high-gain design for prescribed-time regulation of nonlinear systems," *Automatica*, vol. 115, May 2020, Art. no. 108860.

[6] D. Tran and T. Yucelen, "Finite-time control of perturbed dynamical systems based on a generalized time transformation approach," *Syst. Control Lett.*, vol. 136, Feb. 2020, Art. no. 104605.

[7] Y. Chitour, R. Ushirobira, and H. Bouhemou, "Stabilization for a perturbed chain of integrators in prescribed time," *SIAM J. Control Optim.*, vol. 58, no. 2, pp. 1022–1048, 2020.

[8] Y. Orlov, "Finite time stability and robust control synthesis of uncertain switched systems," *SIAM J. Control Optim.*, vol. 43, no. 4, pp. 1253–1271, 2005.

[9] A. Levant, "Robust exact differentiation via sliding mode technique," *Automatica*, vol. 34, no. 3, pp. 379–384, 1998.

[10] J. Davila, L. Fridman, and A. Levant, "Second-order sliding-mode observer for mechanical systems," *IEEE Trans. Autom. Control*, vol. 50, no. 11, pp. 1785–1789, Nov. 2005.

[11] A. Levant, "Higher-order sliding modes, differentiation and output-feedback control," *Int. J. Control*, vol. 76, nos. 9–10, pp. 924–941, 2003.

[12] H. K. Khalil, *Nonlinear Systems*. Upper Saddle River, NJ, USA: Prentice Hall, 2001.

[13] A. F. Filippov, *Differential Equations With Discontinuous Righthand Sides*. Dordrecht, The Netherlands: Kluwer Acad. Publ., 1988.

[14] A. Polyakov, "Nonlinear feedback design for fixed-time stabilization of linear control systems," *IEEE Trans. Autom. Control*, vol. 57, no. 8, pp. 2106–2110, Aug. 2012.

[15] V. I. Utkin, *Sliding Modes in Control and Optimization*, 1st ed. New York, NY, USA: Springer, 1992.

[16] Y. Orlov, Y. Aoustin, and C. Chevallereau, "Finite time stabilization of a double integrator—Part I: Continuous sliding mode-based position feedback synthesis," *IEEE Trans. Autom. Control*, vol. 56, no. 3, pp. 614–618, Mar. 2011.

[17] M. T. Angulo, J. A. Moreno, and L. Fridman, "Robust exact uniformly convergent arbitrary order differentiator," *Automatica*, vol. 49, no. 8, pp. 2489–2495, 2013.